Complementary information relative to the proposal HE-1992: "The study of magnetism of gold-iron alloy based nanoparticles"

The committee likes to see further sample characterisation including the particle size distribution.

In Figure 1 is presented the bright field cross sectional transmission electron diffraction of the sample Au9Fe9 (sequential ion implantation: 60 keV, 9 $\cdot 10^{6}Au^{+}/cm^{+2}$ + 110 keV , 9 $\cdot 10^{6}Fe^{+}/cm^{+2}$). Particle size distribution is very broad being present particles with particle sizes between 20 nm to 3 nm. Largest nanoparticles (10-20 nm size) are mainly dispersed in the projection range of the implanted ions.

In the Figure 2 are represented the Grazing Incidence X-ray diffraction (GIXRD) pattern of this samples. This pattern corresponds to a fcc structure with a lattice parameter of 0.395(1) nm, which is smaller than the Au (0.4071 nm) and larger than that of the high temperature γ-Fe (a=0.3635 nm). Considering a linear relationship between alloy composition and lattice parameter, the Vegard's law, the lattice parameter of the AuFe nanoparticles corresponds to a composition of Au75Fe25.

The GIXRD patterns of three different samples prepared by implanting with different Au/Fe ratio and different total implanted dose are shown in the Figure 3. The Au9Fe3 sample was prepared implanting the same quantity of Au that in the Au9Fe9 but less of Fe (3 $\cdot 10^{6}Fe^{+}/cm^{+2)}$. The Au3Fe3 sample was prepared implanting less quantity of ions 3 $\cdot 10^{6}Fe^{+}$ and Au^{+}/cm^{+2} than the Au9Fe9 but maintaining the Au/Fe ratio = 1. As can be observed only in the case of the Au9Fe9 sample all the peaks of the fcc structure are present and its structure could be well determined. Considering the position of the main peak placed around 40 degree and that all the nanoparticles could have a fcc structure we conclude that the lattice parameter of the Au3Fe3 and Au9Fe3 samples are larger and smaller, respectively than that of the Au9Fe9. In both cases the average grain size is smaller than in the case of the Au9Fe9 sample.The Au3Fe3 sample will be composed by nanoparticles rich in Au. In fact a peak corresponding to surface plasmon resonance typical of gold nanoparticles is observed in the optical absorption spectrum. The magnetic moment per Fe atom is very small 0.4 μ_B and will be interesting to know which is the reason. In the case of the Au9Fe3 the structural data could indicate that the nanoparticles are composed by an alloy more rich in Fe than the Au9Fe9 sample (even if the Fe contain is smaller). However the magnetic moment per Fe atom is 1.4 μ_B, so smaller than that obtained in the Au9Fe9 sample. I point out that Sato et al. (Jpn. J. Appl. Phys. Vol. 41 (2002) pp. L 1–L 3) have obtained nanoparticles of Au-Fe (rich in Au) with the $L1_0$ and $L1_2$ structures and the differences in moment could be related to the different structure. From other point of view a recent work of Brewer et al. (Phys. Rev. Lett 93 (2004) 077205) shows the enhancement of the Fe orbital spin when is dispersed in Au.

One further probe of the growth of the Fe-Au alloy based nanoparticles is their evolution/decomposition under thermal treatments. We have observed that both optical, magnetic and structural properties of annealed samples change only above 500º C. The figure 4 is presented the GIXRD pattern of the Au9Fe9 sample annealed at 600 º C. The peaks can be indexed with two fcc phases with lattice parameters of 0.4035(8) nm and 0.3953(9) nm. This result shows the progressive decreasing of Fe contain in the nanoparticles and growth of a complex nanostructure. The effect of this de-alloying is the presence of the surface plasmon resonance in the optical absorption (Figure 5) and the decrease of the magnetic moment. We ascribe this decreasing to the oxidation of Fe because preliminary TEM studies of the sample annealed at 800º C show the presence of Fe oxides and not of metallic Fe.

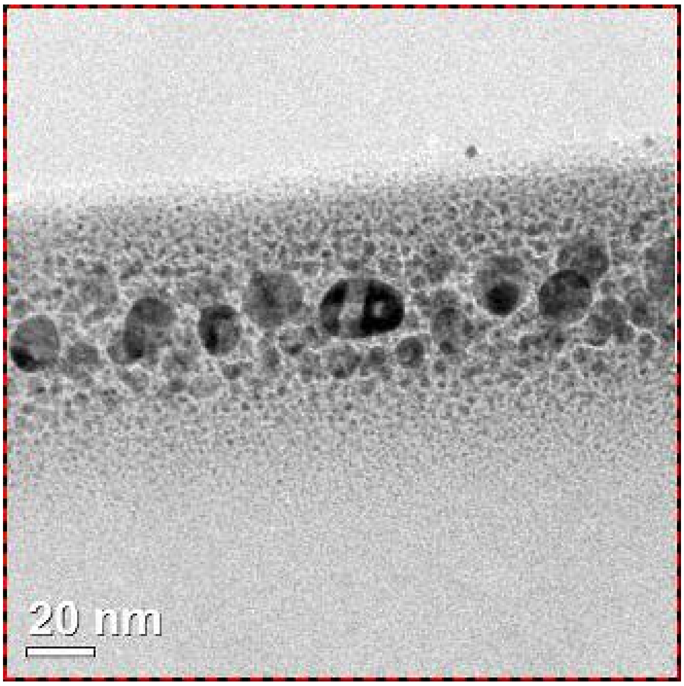

Figure 1. Cross sectional TEM micrograph of the Au9Fe9 sample

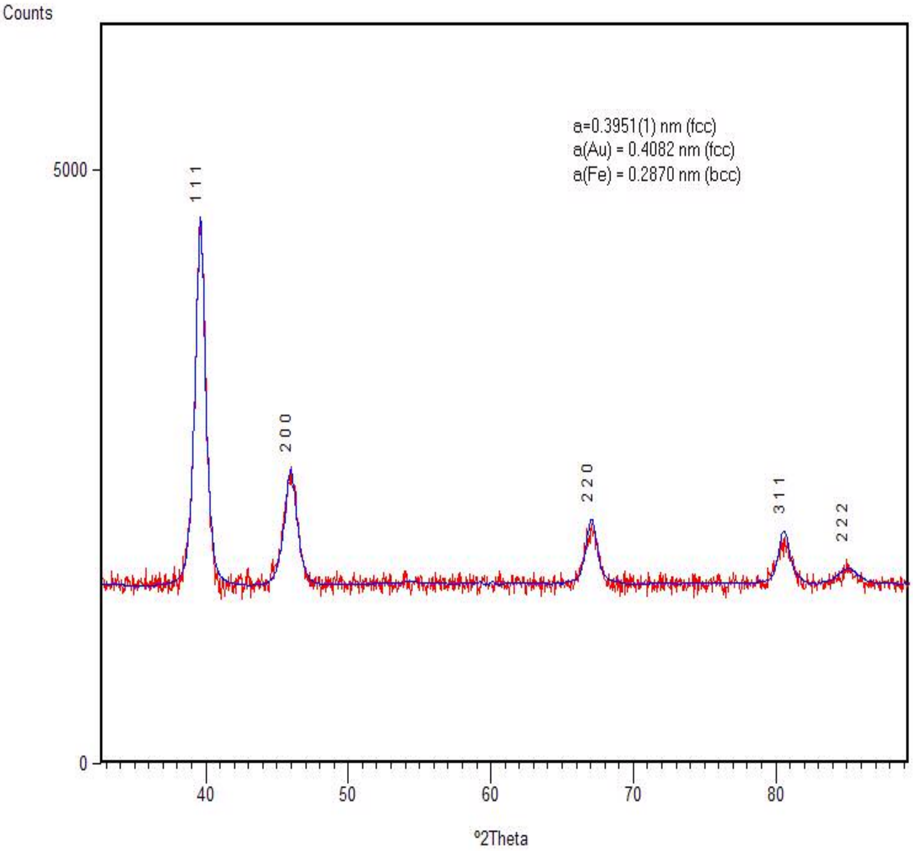

Figure 2. GIXRD pattern of the Au9Fe9 sample

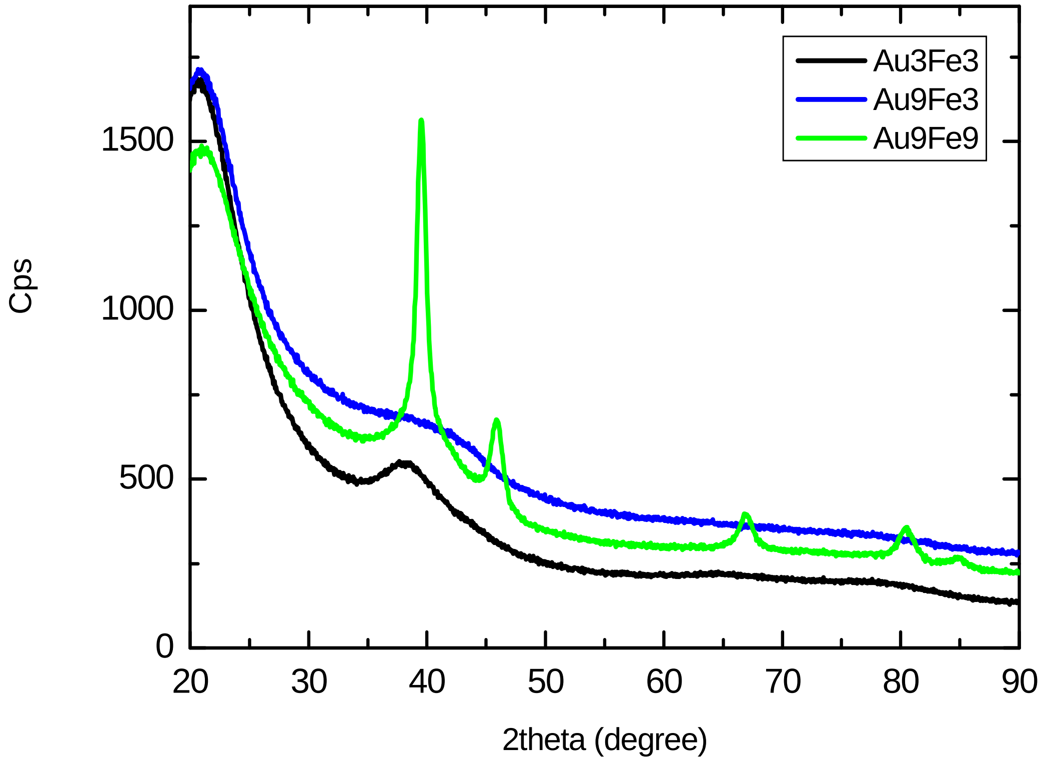

Figure 3. GIXRD of the Au9Fe9, Au9Fe3 and Au3Fe3 samples

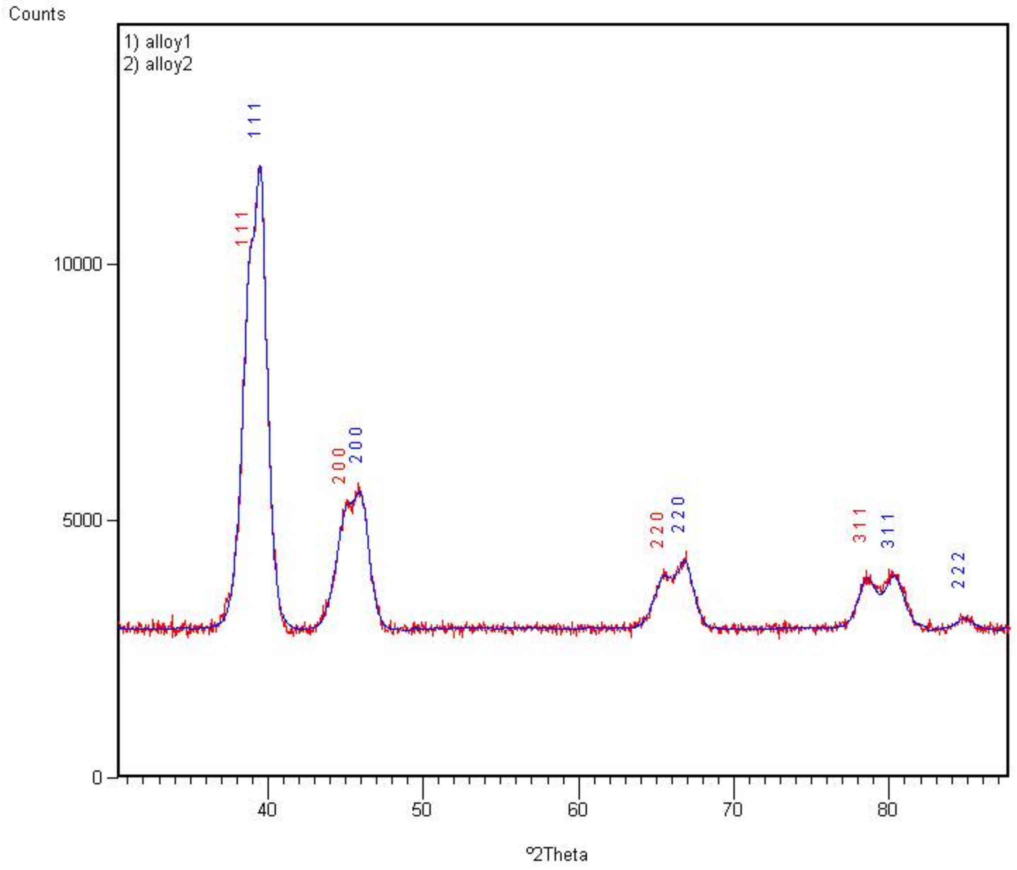

Figure 4. GIXRD of the Au9Fe9 sample annealed at 600° C during 1 hour in H_2(10%)-Ar.

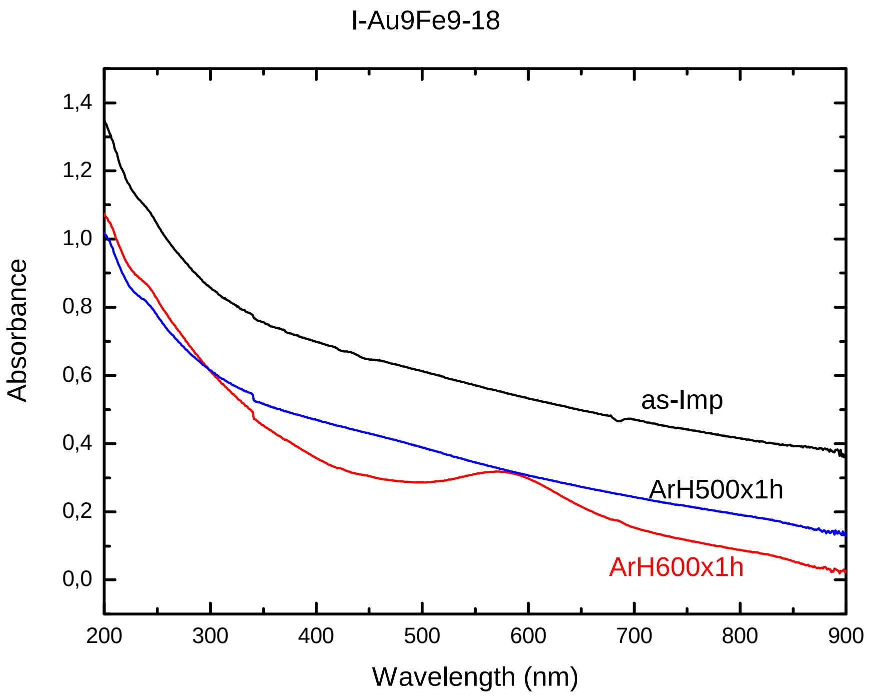

Figure 5. Optical absorption spectra of the Au9Fe9 sample and of the sample annealed at 500° C and 600° C in H_2(10%)-Ar during 1 hour